

Atomic geometry and energetics of vacancies and antisites in cubic boron nitride

W. Orellana^{a)} and H. Chacham

Departamento de Física, Universidade Federal de Minas Gerais, CP 702, 30123-970, Belo Horizonte, MG, Brazil

(Received 29 December 1998; accepted for publication 16 March 1999)

We use first-principles calculations to investigate the atomic geometries and formation energies of vacancies (V_N, V_B) and antisites (B_N, N_B) in cubic boron nitride. We find that V_N and V_B are the most stable defects in p -type and n -type conditions, respectively. They also exhibit intrinsic donor (V_N) and acceptor (V_B) characters, which makes them good candidates for compensation. The equilibrium geometries show large outward breathing relaxations for both vacancies and for B_N , with a slight Jahn–Teller distortion from T_d symmetry. For N_B in neutral and negative charge states, we find an off-center distortion, inducing a negative- U behavior. © 1999 American Institute of Physics. [S0003-6951(99)02120-8]

The current interest in the research on cubic boron nitride (c -BN) resides in its extraordinary thermomechanical properties, ideal for visible as well as ultraviolet optoelectronic and high-temperature devices. c -BN is a wide-band-gap semiconductor which can easily be doped to obtain p -type and n -type materials.¹ This led, ten years ago, to the successful fabrication of a pn -junction diode,² functional up to 600 °C, and later to an ultraviolet light-emitting diode.³ However, the presence of recombination centers associated with native defects or impurities, coupled with the lack of an appropriate technology to achieve high-quality semiconducting samples, have prevented the practical use of c -BN devices.

The high concentration of crystalline defects remains the central problem in the growth methods of BN. Commonly, n -type and p -type conductivities related to defects or impurities have been observed in doped c -BN.^{2,3} In fact, electron paramagnetic resonance (EPR) measurements^{4,5} made in different allotropic form of boron nitride ascribe to the nitrogen vacancy the dominant paramagnetic defect in this material.

There are a few theoretical studies related to native defects in c -BN. Vacancies and/or antisites have been studied with pseudopotential,⁶ tight-binding,⁷ cluster,⁸ and linear augmented plane wave (LAPW)⁹ methods. However, in most of these calculations, the atomic relaxation is restricted to the first-neighbor atoms^{8,9} or simply not considered.⁷

The aim of this work is to present a comparative study of the electronic structure and energetics of antisites and vacancies in c -BN, using first-principles total energy calculations. For each defect, we have determined the fully relaxed atomic geometry in all relevant charge states. Our calculations are based on the density-functional theory,¹⁰ using the supercell approach with 64 atoms per cell, a plane-wave basis set with a kinetic energy cutoff of 60 Ry, and norm-conserving soft Troullier–Martins pseudopotentials.¹¹ For the exchange-correlation functional, we use the generalized gradient approximation (GGA).¹² The integration over the Brillouin zone is performed with one special \mathbf{k} point (the Γ point). The

geometry optimization is obtained by calculating Hellmann–Feynman forces on the nuclei. The atomic positions are considered converged when the forces on the atoms are less than 0.05 eV/Å. A detailed description of the computational method is given in Ref. 13.

The formation energies of native defects in c -BN are calculated as a function of the chemical potentials of nitrogen and boron. For charged systems, the formation energy also depends on the position of the Fermi level. Thus, for a defect in the charge state q , the formation energy is given by¹⁴

$$E_{\text{form}}(q) = E_t(q) - n_N \mu_N - n_B \mu_B + q(\mu_e + E_v), \quad (1)$$

where E_t is the total energy of the defect derived from the supercell calculation, n_N (n_B) is the number of N (B) atoms in the supercell, and μ_N (μ_B) is the corresponding chemical potential. μ_e is the electronic chemical potential or the position of the Fermi level relative to the valence band edge, and E_v is the energy of the top of the valence band for bulk c -BN. The atomic chemical potentials can vary over a range given by the heat of formation of c -BN, defined as $H_f = E_{B(\text{bulk})} + E_{N(\text{bulk})} - E_{c\text{BN}(\text{bulk})}$, which we calculated in 3.0 eV. Additionally, they are constrained by the equilibrium condition: $\mu_N + \mu_B = \mu_{c\text{BN}(\text{bulk})}$. Upper bounds for μ_N and μ_B are the precipitation limits on bulk phases: $\mu_N < \mu_{N(\text{bulk})}$ and $\mu_B < \mu_{B(\text{bulk})}$, which are calculated from solid nitrogen (α -N₂) and metallic boron (α -B), respectively. For bulk c -BN, we find an equilibrium lattice constant $a_0 = 3.617$ Å and a bulk modulus $B = 3.80$ Mbar,¹⁵ which are in good agreement with the experimental values ($a_0 = 3.615$ Å and $B = 3.69$ Mbar).¹⁶ For the band structure, we obtain an indirect gap ($\Gamma_{15}^v \rightarrow X_1^c$) of 4.8 eV. α -N₂ has a face-centered-cubic (fcc) structure with four N₂ molecules per unit cell. We find an equilibrium lattice constant $a_0 = 5.934$ Å, within 5% of the experimental value (5.65 Å).¹⁷ α -boron has a rhombohedral structure formed by B₁₂ icosahedra which can be represented by a 36-atoms hexagonal unit cell. To calculate α -B, we fix the c/a ratio of the hexagonal cell to its experi-

^{a)}Electronic mail: wmomunoz@fisica.ufmg.br

TABLE I. Change in the defects geometry with charge state for boron and nitrogen vacancies. Units are in percent with respect to the unrelaxed defects. Δd_1 is the mean variation on the distance between the vacancy center and the first-neighbor atoms. Δd_2 is the mean variation on the distance between first- and second-neighbor atoms. E_r is the relaxation energy, in eV.

Charge	V_N			V_B		
	Δd_1	Δd_2	E_r	Δd_1	Δd_2	E_r
3+	19.8	-5.7	2.79			
2+	15.4	-4.8	1.79			
1+	7.6	-2.9	0.72	10.8	-4.0	1.83
0	7.7	-2.9	1.19	10.5	-4.3	2.14
1-				10.4	-4.9	2.29
2-				10.3	-5.8	2.57
3-				10.3	-6.5	2.70

mental value (~ 2.56). We find an equilibrium lattice constant $a = 5.122 \text{ \AA}$, within 5% of the experimental value (4.908 \AA).¹⁸

Our results for the equilibrium geometries and relaxation energies of boron and nitrogen vacancies in different charge states are summarized in Table I. In both vacancies, we find large outward breathing relaxations of the nearest-neighbor atoms, with slight distortions from the T_d symmetry for every charge state investigated. We also note that V_N suffers a more drastic relaxation with the charge state as compared with V_B . The electronic structure of native defects in *c*-BN is presented schematically in Fig. 1. In the figure, we show the positions of the defect-induced one-electron states in the band gap, for the neutral vacancies and antisites. For V_N^0 , we find a fully occupied *s*-like a_1 state in the band gap close to the valence band edge, and a doublet state slightly split into singlets, lying as an *e*-like resonance in the bottom of the conduction band. Because this resonance is singly occupied, the neutral charge state is unstable, and V_N only exists in donor states. For V_B^0 , we find a *p*-like t_2 state in the lower part of the band gap, which also shows a slightly split into singlet states. This t_2 state is half occupied, thus acting as a triple acceptor. The small splitting of the partially filled degenerate levels indicates a very small Jahn–Teller (JT) effect in the neutral vacancies. The difference in energy between split levels is less than 10 meV.

The equilibrium geometry for B_N^0 shows an outward breathing relaxation of the neighboring B atoms, with a

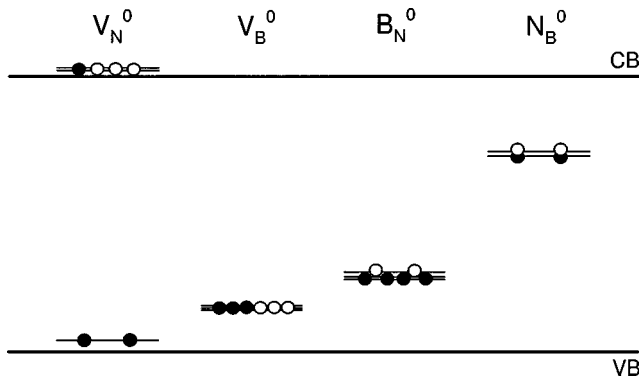


FIG. 1. Schematic representation of one-electron levels in the band gap induced by vacancies and antisites in *c*-BN in neutral charge states. The filled circles indicate electrons and the open circles indicate holes.

small distortion of the B antisite along the [100] direction (about 0.03 \AA from the N-site). The distance between B_N and its first neighbors is 5.2% larger than in the unrelaxed system, while the distances between first and second neighbors are 0.2% shorter. No distortion along the [111] direction has been detected. We observe only small distortions of the B antisite for every charge state investigated. The electronic structure for B_N^0 (Fig. 1) shows a *p*-like t_2 state in the gap, which is occupied with four electrons. This state also splits into singlet states, due to the small JT distortion.

For N_B^0 , we observe an off-center distortion of the N antisite along the [100] direction, with a minimum at 0.35 \AA from the B-site. The N antisite binds to two neighboring N atoms, forming a bridge structure with equal N–N bond lengths of 1.41 \AA , and an angle of 122° between the bonds. For the negative charge states, we also find the same distortions which are characterized by large lattice relaxations. However, for positive charge states, we observe a breathing relaxation, preserving the T_d symmetry. The gap levels for N_B^0 shown in Fig. 1 correspond to the off-center configuration with C_{2v} symmetry. We find a fully occupied *s*-like a_1 state in the upper part of the band gap, close to an empty a_1 state. The difference in energy between these states is 0.07 eV. The empty a_1 state originates from the split of a t_2 gap state of the defect in T_d symmetry.

The distortions observed in the B_N^0 and N_B^0 defects were checked with calculations including four special \mathbf{k} points.¹⁹ No additional distortions or changes in the equilibrium positions with respect to the calculation with one \mathbf{k} point were found. Moreover, the difference in total energy between the two \mathbf{k} -point samples is less than 0.07 eV/B–N pair.

In Fig. 2(a), we show our results for the formation energies of native defects as a function of the Fermi energy (μ_e) for nitrogen-rich conditions. In this figure, the slopes of the line segments correspond to the charge states of the defects. Changes in the slopes indicate transition states, which are represented by symbols. The range of variation for μ_e is chosen to be the value of the experimental gap (6.4 eV).²⁰ We observe that for *p*-type conditions (Fermi energy close to the top of the valence band), V_N^{3+} has the lowest formation energy and can be considered as the dominant defect. N_B^{2+} also exhibits low formation energies, comparable to those of V_N^{3+} . On the other hand, for semi-insulating and *n*-type conditions (Fermi energy near the middle of the gap and close to the bottom of the conduction band, respectively), V_B^{3-} exhibits the lowest formation energy, and hence is a dominant defect on *c*-BN.

The formation energies for boron-rich conditions are shown in Fig. 2(b). Similar to the N-rich case, the vacancies are the dominant defects. V_N^{3+} and V_B^{3-} have the lowest formation energies in *p*-type and *n*-type conditions, respectively. We also note that the boron antisite exhibits low formation energies in the entire range of the band gap, which are comparable to those of the vacancies. In fact, B_N has the lowest formation energy for $2.4 < \mu_e < 3.8 \text{ eV}$. Therefore, the boron antisite should also be considered as a dominant defect in B-rich *c*-BN.

Recent core-level photoabsorption studies on hexagonal BN thin films²¹ indicate that ion bombardment produces *sp*³-bonded material with the presence of nitrogen intersti-

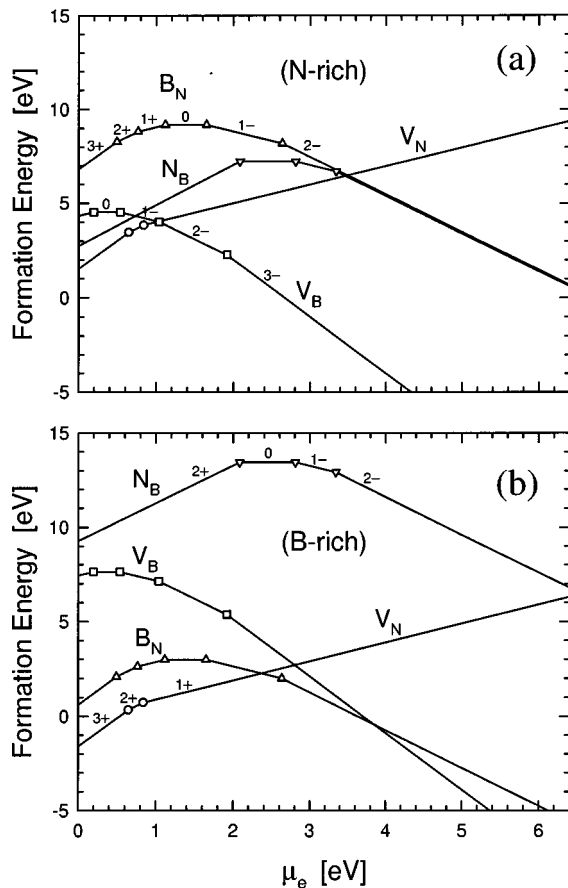


FIG. 2. Formation energies, as a function of the Fermi level (μ_e), for vacancies and antisites in *c*-BN. (a) For nitrogen-rich condition, $\mu_N = \mu_{N(\text{bulk})}$. (b) For boron-rich condition, $\mu_B = \mu_{B(\text{bulk})}$. The slopes of the line segments characterize to defects charge states, and the symbols characterize transition states.

tials, while the remaining sp^2 material exhibits nitrogen vacancies. However, no evidence of boron vacancies is found. The relevant energetics for the defect production by ion bombardment can be obtained by the comparison between the formation energy E_1 of a $V_B + B_i$ distant pair and the formation energy E_2 of a $V_N + N_i$ distant pair. We obtain $E_1 > E_2$ for *p*-type condition and $E_1 < E_2$ for *n*-type condition. Therefore, we predict that if experiments similar to those of Ref. 21 are made for cubic BN, nitrogen vacancies would be produced in *p*-type materials and boron vacancies would be produced in *n*-type materials, unless the cross section for nitrogen–boron collisions is too small.

We now turn our attention to other important subjects derived from our calculations. We find that the nitrogen vacancy in *n*-type *c*-BN shows high formation energies (>6 eV). Therefore, the observed *n*-type conductivity³ usually associated to the nitrogen vacancy would imply either in a nonequilibrium incorporation of this defect or in the incorporation of a donor-like impurity with lower formation energy. According to our equilibrium calculation, the nitrogen vacancy should not be responsible for the *n*-type conductivity. The same picture has also been suggested for V_N in GaN.²²

Additionally, our results show that N_B^+ is never stable, which characterizes a negative- U behavior for this defect, where $U = E^{(+/0)} - E^{(2+/+)} \approx -0.7$ eV. The origin of this

negative- U behavior is related to the off-center distortion of the nitrogen antisite in the neutral charge state. The $(2+/0)$ transition, located at 2.1 eV from the top of the valence band, is characterized by a large lattice relaxation, with an energy gain of about 2 eV.

Finally, EPR measurements have reported paramagnetic defects in bulk⁴ and thin-film⁵ boron nitride, which are commonly associated to V_N in neutral charge state. Our results show that V_N only exists in positive charge states, supporting that V_N^{2+} , instead V_N^0 , should be the paramagnetic center associated to the nitrogen vacancy in *c*-BN.

In summary, we have found, based on first-principles calculations, that nitrogen and boron vacancies are the dominant defects in nonstoichiometric *c*-BN for *p*-type and *n*-type conditions, respectively. The vacancies also show intrinsic donor (V_N) and acceptor (V_B) characters which makes them the main candidates for the experimentally observed dopant compensation. According to our calculation the high formation energies observed for V_N in *n*-type conditions exclude it as a source of *n*-type conductivity.

This work was supported by the Brazilian agencies FAPEMIG and CNPq. The calculations were performed at CENAPAD-MG/CO. The authors acknowledge R. W. Nunes for critical reading of the manuscript.

- ¹R. H. Wentorf, Jr., J. Chem. Phys. **36**, 1990 (1962).
- ²O. Mishima, J. Tanaka, S. Yamaoka, and O. Fukunaga, Science **238**, 181 (1987).
- ³O. Mishima, K. Era, J. Tanaka, and S. Yamaoka, Appl. Phys. Lett. **53**, 962 (1988).
- ⁴F. Zhang and G. Chen, Mater. Res. Soc. Symp. Proc. **242**, 613 (1992).
- ⁵M. Fanciulli and T. D. Moustakas, Physica B **185**, 228 (1993).
- ⁶Y. Bar-Yam, T. Lei, T. D. Moustakas, D. C. Allan, and M. P. Teter, Mater. Res. Soc. Symp. Proc. **242**, 335 (1992).
- ⁷V. A. Gubanov, Z. W. Lu, M. Klein, and C. Y. Fong, Phys. Rev. B **53**, 4377 (1996).
- ⁸P. Piquini, R. Mota, T. M. Schmidt, and A. Fazzio, Phys. Rev. B **56**, 3553 (1997).
- ⁹J. L. P. Castineira, J. R. Leite, L. M. R. Scolfaro, R. Enderlein, H. W. L. Alves, and J. L. A. Alves, Radiat. Eff. Defects Solids **146**, 49 (1998).
- ¹⁰P. Hohenberg and W. Kohn, Phys. Rev. **136**, B864 (1964); W. Kohn and L. J. Sham, Phys. Rev. **140**, A1133 (1965).
- ¹¹N. Troullier and J. L. Martins, Phys. Rev. B **43**, 1993 (1991).
- ¹²J. P. Perdew, J. A. Chevary, S. H. Vosko, K. A. Jackson, M. R. Pederson, D. J. Singh, and C. Fiolhais, Phys. Rev. B **46**, 6671 (1992).
- ¹³R. Stumpf and M. Scheffler, Comput. Phys. Commun. **79**, 447 (1994).
- ¹⁴S. B. Zhang and J. E. Northrup, Phys. Rev. Lett. **67**, 2339 (1991).
- ¹⁵Determined by fitting the total energy to the Murnaghan's equation of state.
- ¹⁶E. Knittel, R. M. Wentzcovitch, R. Jeanloz, and M. L. Cohen, Nature (London) **337**, 349 (1989).
- ¹⁷T. H. Jordan, H. W. Smith, W. E. Streib, and W. N. Lipscomb, J. Chem. Phys. **41**, 756 (1964).
- ¹⁸B. F. Decker and J. S. Kasper, Acta Crystallogr. **12**, 503 (1959).
- ¹⁹D. J. Chadi and M. L. Cohen, Phys. Rev. B **8**, 5747 (1973).
- ²⁰R. M. Chrenko, Solid State Commun. **14**, 511 (1974).
- ²¹I. Jimenez, A. F. Jankowski, L. J. Terminello, D. G. J. Sutherland, J. A. Carlisle, G. L. Doll, W. M. Tong, D. K. Shuh, and F. J. Himpsel, Phys. Rev. B **55**, 12025 (1997).
- ²²J. Neugebauer and C. G. Van de Walle, Phys. Rev. B **50**, 8067 (1994).